JOURNAL OF MATERIALS SCIENCE 28 (1993) 5199–5206

On-line ultrasonic monitoring and modelling of radiation-induced structural changes in polymethyl methacrylate

B. BRIDGE
School of Electrical, Electronic and Information Engineering, South Bank University, 103 Borough Road, London SE1 0A, UK

Structural changes in polymethyl methacrylate (PMMA, monomer formula $C_2H_2CH_3COOCH_3$) induced by ^{60}Co radiation have been detected by means of on-line monitoring of increases in the attenuation of 10 MHz longitudinal ultrasound. Attenuation changes first became noticeable at a dose of 15 kGy and had increased by 75% at the maximum dose of 36.5 kGy. A theoretical upper bound to structural relaxation loss induced by radiation has been calculated. As a consequence it was then possible to show that at the dose levels encountered, the additional loss was attributable mainly to collective motions involving many atoms and of low attempt frequencies, rather than to the relaxation of individual atoms or structural groupings. The theory proposes an attenuation change proportional to the 5/3th power of the dose, which is in excellent agreement with experiment. It is suggested that on-line monitoring of ultrasound loss could be a sensitive diagnostic test of the onset of unwanted structural change during the practice of food preservation by the use of irradiation.

1. Introduction

Studies of the effects of high-energy particle, X, or gamma radiation on the ultrasonic properties of polymers and glasses are long established but rare, and only slightly less so for other solids. Typical examples are given by the experiments of Ritchie *et al.* on gamma irradiated iron [1], Beretz *et al.* on Ag–Zn alloys subject to fast electrons, reactor neutrons and gamma rays [2], Fraser on the gamma irradiation of crystalline silica [3], Strakna on neutron-bombarded silica glass [4], and Callens *et al.* on gamma irradiated polyvinylidine fluoride [5]. Invariably, this previous work has been carried out "off-line" i.e. ultrasonic/internal friction properties of samples subject to varying radiation doses have been measured and compared only after the samples have been removed from the radiation enclosure. In an "on-line" study there are no troublesome corrections to be made for the differences in the acoustic bond between the transducers and different samples. Thus much smaller changes in ultrasonic attenuation can be detected. Another advantage is that a continuum of radiation doses can be studied. Finally, acknowledging that ultrasound attenuation is a sensitive indicator of microstructural change, slight structural differences between samples will not mask radiation dose effects.

The novel on-line study described here became possible because of a rare opportunity: the availability on the same premises of ultrasonic equipment and a high-intensity ^{60}Co enclosure with electronic links between the interior of the enclosure and a radiation-free control and observation room. The source intensity of 370 GBq (10 Curie) was at least two orders of magnitude less than what is ordinarily used for medical purposes such as tissue and cell damage studies, or in food irradiation for bacteria destruction. However, comparable sample dose rates were possible because the small samples employed could be sited within a millimetre or two of the ^{60}Co pellet.

2. Experimental procedures

The shielded enclosure, approached by a labyrinth entrance had dimensions of 5 m × 5 m, a height of 2.3 m, and contained an array of 50, 50 Ω coaxial through-connections to a control laboratory via cables running in an underground duct. Walls, floors and ceiling constructed of 1.3 m thick standard density concrete permitted the source to be located anywhere within the enclosure. Multiple power points were available in the enclosure walls to allow *in situ* operation of electronic instrumentation. However to avoid any possibility of radiation damage to the electronic components, all ultrasonic instrumentation except the transmitter/receiver transducer was kept in the control room.

A spring-loaded sample holder was constructed to maintain a parallel-sided polymer disc (5 mm thick and 10 mm diameter) in contact with a commercial compression wave transducer (Krautkramer 10 MHz, 10 mm diameter). A conical tipped brass snout, which contained the ^{60}Co source in its wound out position, was supported with the tip in contact with the circumference of the polymer disc so that the axes of the

0022–2461

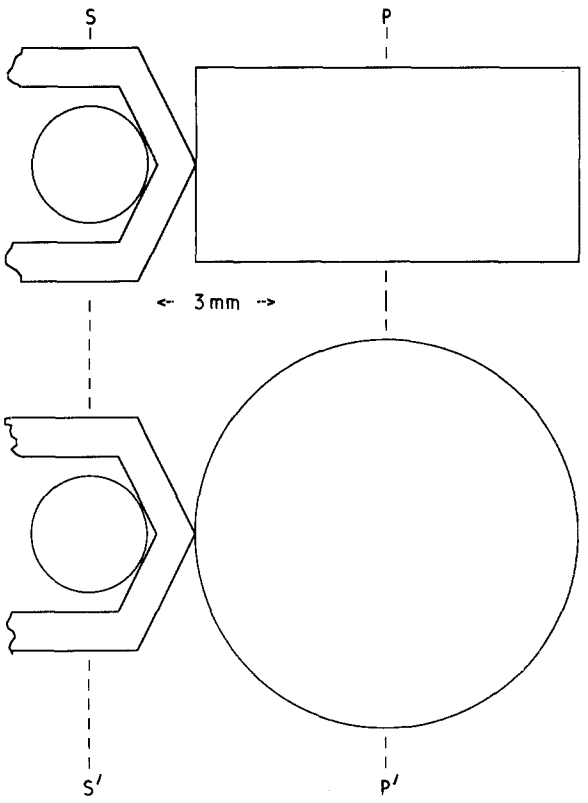

Figure 1. Configuration of source pellet (small circle), brass tube with conical snout which locates the pellet, and the polymer disc specimen (rectangle and large circle indicate orthogonal sections through the centre of the disc).

snout and the disc were orthogonal (Fig. 1). Using controls located in the labyrinth entrance the source was wound into the snout from a class B container stored under the floor of the enclosure. In the wound out position the perimeters of the 3 mm diameter source pellet and the sample disc were separated at their closest point by about 2.5 mm. In the control room a broad band pulser-receiver was employed (Panametrics 5052PR, 35 MHz bandwidth) and r.f. echo patterns were displayed on a 100 MHz cathode ray oscilloscope. The single coaxial link between the pulser-receiver and the transducer was about 14 m long. No serious distortion or attenuation of received signals (nominally 1 μs duration and 10 MHz central frequency) along the link was experienced.

Attenuation measurements were made at regular time intervals by comparing the heights of successive echoes. Mean values were obtained by using the first, second and third echoes, the attenuation levels being too high for higher order echoes to be observable. Measurements on single echoes alone were considered too unreliable because of the possibility of scattered radiation affecting the properties of the bonding fluid or (less likely) the ceramic transducer element. The attenuation data are considered to be relatively (rather than absolutely) accurate to $\pm$ 0.1 dB. An irradiation period of about 24 h was used. The attenuation increased monotonically with irradiation time, and was approximately double its initial value at the end of the run (Fig. 2).

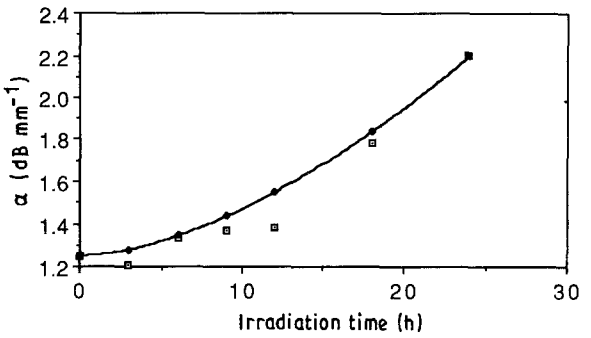

Figure 2. The effect of ^{60}Co radiation on the attenuation coefficient, α, of 10 MHz ultrasonic compressional waves propagating in polymethyl methacrylate. (⊡) Experimental data points and the experimental errors, which are $\pm$ 0.1dB mm^{-1}. (◆, ■, ——) A theoretical fit of Equation 29 to the experimental data on the assumption that the mean polymer chain length $\langle n_f \rangle$ is inversely proportional to the radiation dose. The theory proposes that the attenuation change is proportional to the 5/3th power of $1/\langle n_f \rangle$, and therefore to the 5/3th power of the dose. Dose rate: 1.52 kGy h^{-1}.

3. Dose calculations

To calculate a mean specimen dose rate we need to evaluate a quantity, r, the separation of an equivalent point source and point specimen. From inspection of Fig. 1, about 80% of source photons will start out from points within $\pm$ 1 mm of the circular slice SS' through the centre of the source. This slice is located 2.5 mm from the point of the specimen nearest the source. Next consider a parallel slice PP' through the centre of the sample. Some 50% of the sample volume passed through by the source photons lies within $\pm$ 2 mm of the slice. Thus to a first approximation, the distance from the source centre to the specimen centre, which was 7.5 mm, is a reasonable estimate for r.

Because the Curie unit is 3.76×10^{10} disintegrations per second, the photon flux in the point specimen, assuming a 10 Curie point source, is $2 \times 3.76 \times 10^{11}/4\pi \times 7.5 \times 7.5 = 1.06 \times 10^{9}$ mm^{-2}s^{-1}, as two photons are emitted in cascade during each disintegration. ^{60}Co photons interact with matter to produce free electrons predominantly by Compton scattering, in which photons are deflected with some energy loss; and by photoelectric absorption in which the photon completely disappears. The linear attenuation coefficients for both interaction processes decrease with increasing photon energy, and the respective attenuation coefficients are proportional to the atomic number (i.e. roughly proportional to material density) and to the fourth or fifth power of the atomic number. For light materials such as the polymer under study, the photoelectric coefficient becomes smaller than the Compton coefficient for energies above 100 keV and at 1 MeV it is completely negligible in comparison [6]. Thus for ^{60}Co photons the linear attenuation coefficient of the polymer derives entirely from Compton scattering. We shall take for its value

$$\mu_C = 7.40 \times 10^{-3} \text{ mm}^{-1} \quad (1)$$

where the subscript C denotes the Compton effect. This value has been extrapolated from a tabulated

value of 8.16×10^{-3} mm^{-1} at 1 MeV [7]. The extrapolation has been obtained by comparison with linear extrapolations between 1 and 1.5 MeV attenuation data for carbon and hydrogen [8], as there was insufficient direct data for the polymer. As the attenuation coefficient is much less than unity, over a 1 mm path length the number of photons removed from the primary beam, N_C, is given by the product of the attenuation coefficients and the local beam flux. Thus in our point model specimen we have

$$N_C = 7.84 \times 10^6 \text{ s}^{-1}\text{mm}^{-3} \quad (2)$$

The mean free path of the scattered photons is very large compared with the actual specimen size. Thus once a photon has been Compton scattered it is unlikely to do so again on a subsequent occasion. So only those photons which have interacted for the first time within a given small volume will lead to ionization within that volume. Thus the number of ionizations per second per cubic millimetre of specimen caused directly by the photons is simply N_C. In addition these free electrons cause further ionizations by virtue of their momentum. The mean free path of fast free electrons is only fractions of a millimetre [9] so that the subsequent ionization that they cause occurs within the same region as the initial ionization event. It thus follows that all the energy of the Compton free electrons is available for ionization within the sample volume of interest. The mean energy imparted to these electrons, averaging over all orientations, and obtained by numerical integration [10], is 0.38 MeV. So that taking a mean ionization energy of 12 eV, the mean of the values for the hydrogen and carbon atoms, there are $0.38 \times 10^6/12 = 3.17 \times 10^4$ ionizations per Compton interaction. Correspondingly the total ionization rate per cubic millimetre of specimen is

$$3.17 \times 10^4 \, N_C = 2.49 \times 10^{11} \text{ s}^{-1} \quad (3)$$

During an experimental run of 24 h there are

$$N_i = 2.15 \times 10^{16} \text{ ionizations/mm}^3 \quad (4)$$

whilst there are

$$N_b = 1.13 \times 10^{20} \text{ bonds/mm}^3 \quad (5)$$

Therefore, about 1 in 5000 bonds are ruptured and re-formed, i.e. 0.02% of all bonds.

4. General considerations on ultrasonic loss in polymers

In polymers and glasses the dominant mechanism of ultrasonic attenuation at most temperatures, including temperatures well below the glass transition temperature, is structural relaxation. More specifically we mean the thermally activated motion of structural groupings, (translational motion of single atoms or segments of main chain, rotational motion of side groups of several atoms, etc.) across potential barriers. A characteristic feature of a totally or partly amorphous material is the presence of substantial volume distributions of potential barriers of heights far less than bond ionization energies. This is why the structural relaxation losses in these materials can be large even at low temperatures. In contrast, in a perfect crystal the only mechanism for structural relaxation is thermally activated ionization. Low potential barriers can be produced by point lattice defects and dislocations in crystals, i.e. by any deviation from perfect crystallinity. However, the structural relaxation losses in such cases will be much lower than in a polymer, unless a crystal is so deformed as to be classifiable as being virtually amorphous.

A particle which can move across a potential barrier between two wells but is otherwise constrained, is commonly described as a two-well system, and on account of the associated relaxation loss it is frequently described more concisely as a "loss centre". For a single loss centre the internal friction takes the form [11]

$$Q^1 = (-D^2/\rho c^2)(\mathrm{d}/\mathrm{d}\Delta)[1 + \exp(\Delta/kT)]^{-1} \times [\omega\tau/(1 + \omega^2\tau^2)] \quad (6)$$

where D is the deformation potential [12], ρ is the density, c is the acoustic phase velocity, Δ is the well asymmetry, i.e. separation of the two-well minima, kT has its usual meaning, ω is the angular frequency, and τ is the relaxation time given by [11]

$$\tau = \tau\exp(V/kT)\operatorname{sech}(\Delta/kT) \quad (7)$$

where V is the barrier height measured from a potential level half-way between the two-well minima, and τ is the reciprocal of the classical attempt frequency, i.e. it is the classical period between impacts of a particle in one well on the barrier walls. The notation used here for barrier height, relaxation time and reciprocal classical attempt frequency differs from the more usual notation employed [11, 12]. The change has been deliberate to avoid the cumbersome use of double subscripts later in the paper.

The deformation potential $D = \delta\Delta/\delta\varepsilon$, where ε is the elastic strain, i.e. the potential is equal to the shift in the separation of the two-well minima that takes place when the local strains experienced by the two minima differ by an amount $\delta\varepsilon$. More generally, D is the change in local potential experienced by a particle, i.e. the change in its free energy, when it moves through a distance over which the local strain changes by an amount $\delta\varepsilon$. This more general definition will be seen to be advantageous when we consider the case of a two-well system degenerating into a single well, in the following paragraph. According to the theory of Bridge and Patel [12], for a motion involving a single atom constrained by nearest neighbour atoms

$$D \approx qA y\cos\phi \approx 2qy\cos\phi/n_a x \quad (8)$$

where $q = pc^2$, the appropriate elastic modulus, A is the effective cross-sectional area of the two-well system, y is the separation of the two-well minima, x is the longitudinal dimension of the system, i.e. about two atomic spacings (bond lengths), n_a is the number of atoms per unit volume ($n_a \approx 2/Ax$), and ϕ denotes the orientation of the well axes with respect to the wave propagation direction. One could equally well make out a case for using N_b instead of n_a in Equation

8 but it scarcely matters in an order of magnitude calculation. Coincidentally, the two values are the same in PMMA because the number of atoms and bonds per monomer unit are the same, i.e. 16. Thus the maximum possible value of the deformation potential is obtained when y takes on its maximum possible value $= x$ and $\cos\phi = 1$, i.e.

$$D_{max} \approx 2q/n_a = 2\rho c^2/n_a \quad (9)$$

When averages of D are taken over many two-well systems, which will have random orientations, the factor of 2 in Equations 8 and 9 disappears. Taking for PMMA, $\rho = 1171\ \mathrm{kg\,m^{-3}}$, $c = 2600\ \mathrm{m\,s^{-1}}$, and a value of $1.129 \times 10^{29}\ \mathrm{m^{-3}}$ for n_b (obtained from the monomer formula), one obtains

$$D_{max} = 0.9\ \mathrm{eV} \quad (10)$$

The case of $V \to 0$, when two wells degenerate into one, is particularly interesting in the present context. What happens to Q^{-1} in this limit depends on D, which in turn depends crucially on the well shape via the ratio y/x. All other quantities in Equation 8 remaining the same, the quantity D increases with y, the maximum distance that the relaxing particle moves through the acoustic stress field, under thermal excitation. For a highly anharmonic, i.e. flat-bottomed, well the value of y is substantial, i.e. a significant fraction of one atomic spacing just as in the case of $V \gg 0$. Correspondingly, y/x and D will take on a significant value, i.e. of the same order of magnitude as its value (1 eV) for a well of substantial barrier height. As discussed subsequently in Section 6, the single flat-bottomed well may be an appropriate description of relaxation loss produced by the collective motion of chains. For a case of single harmonic wells the amplitude, y, of thermal motions at a given temperature is obviously far less than in the previous case, so that $y/x \ll 1$, D is now relatively very small, and correspondingly, so is Q^{-1}. That there is any loss at all is a consequence of the local nature of the model used to derive Equation 6, in which vibrations of neighbouring harmonic wells are considered to be independent. In a continuum (lattice vibration) approach no overall loss at all results from harmonic vibrations, i.e. in quasi-particle language phonon-phonon interactions stem only from vibrational anharmonicity.

In the most general case a polymer may be considered to have an ensemble of different types of barrier, distinguished by the kind of structural grouping involved, and each type having a continuous distribution of heights. Taking these distribution functions to be of the general form [13]

$$n(V) = V^{-1}\exp(-V/V) \quad (11)$$

where V is the arithmetical mean of V, assuming a relatively broad range of asymmetries, and adopting the common condition that $\omega\tau \ll 1$, an analytical solution of the integrals over terms like Equation 7 are obtained [12, 13], which makes a suitable starting point for a tractable discussion. Thus one obtains an internal friction function of the relatively simple form

$$Q^{-1} = \Sigma[\pi D_i^2 n_i kT(\omega\tau_i)^{(kT/V_i)}]/(4\rho c^2 V_i^2) \quad (12)$$

where the subscript i denotes a summation over i types of barrier and n_i is the number of loss centres per unit volume having the barrier type i. For each barrier type the deformation potential and the attempt frequency have been taken as constants across the barrier height distribution because variations in these quantities have a much smaller effect on the internal friction than have barrier height changes. Usually even with T as high as T_g, $kT/V_i \ll 1$, so that the frequency dependence of Q^{-1} is very weak, i.e. the linear attenuation coefficient per unit length varies as the first power of the frequency so that the loss can be mistakenly attributed to a hysteresis mechanism.

The permanent attenuation change produced by the irradiation implies that changes in one or more of the group of quantities n_i, V_i, τ_i, has been produced. This, in turn, suggests that changes have arisen in the relative positions of substantial numbers of atoms throughout the polymer sample. Photon radiation, unlike neutron radiation, does not transfer momentum directly to nuclei and therefore cannot be solely responsible for the translational motion of atoms. What happens is that by ionization, i.e. by the release of free electrons, atomic bonds are ruptured, allowing some atoms or groups of atoms to move subsequently by thermal activation. When the free electrons are subsequently recaptured and bonds are re-formed the free atomic movements become frozen in, and the net effect of the radiation is thus to make the polymer structure even more amorphous (PMMA has no crystalline component) than hitherto. To give specific examples, if a bond between a main chain and a side group is broken, the group as a whole is free to move translationally. If a single bond in a main chain is broken, then extra vibrational degrees of freedom are introduced, whilst if two bonds in the same main chain are broken, extra translational degrees of freedom arising from the chain segment are created.

5. Upper theoretical bound to radiation-induced ultrasonic loss

The qualitative picture just described gives few clues, considered by itself, as to how n_i, V_i, τ_i and Q^{-1} are affected quantitatively by radiation. Inspection of Equations 6, 7 and 12 admit the possibility of a change in a V, V or τ value being able to produce a positive or negative contribution to Q^{-1}. Thus as a matter of general principle it is plausible that irradiation can either increase or decrease an ultrasonic loss caused by stuctural relaxation. However, we can estimate the maximum possible attenuation that can be introduced into the sample assuming that the maximum number of loss centres has been produced (Fig. 3), as follows. If, for simplicity, we assume a single distribution function, then assuming that Equation 12 holds, i.e. $\omega\tau \ll 1$, a maximum in the variation of Q^{-1} with respect to V at constant T occurs, and is defined by

$$V_{max} = -(kT/2)\ln\omega\tau \quad (13)$$

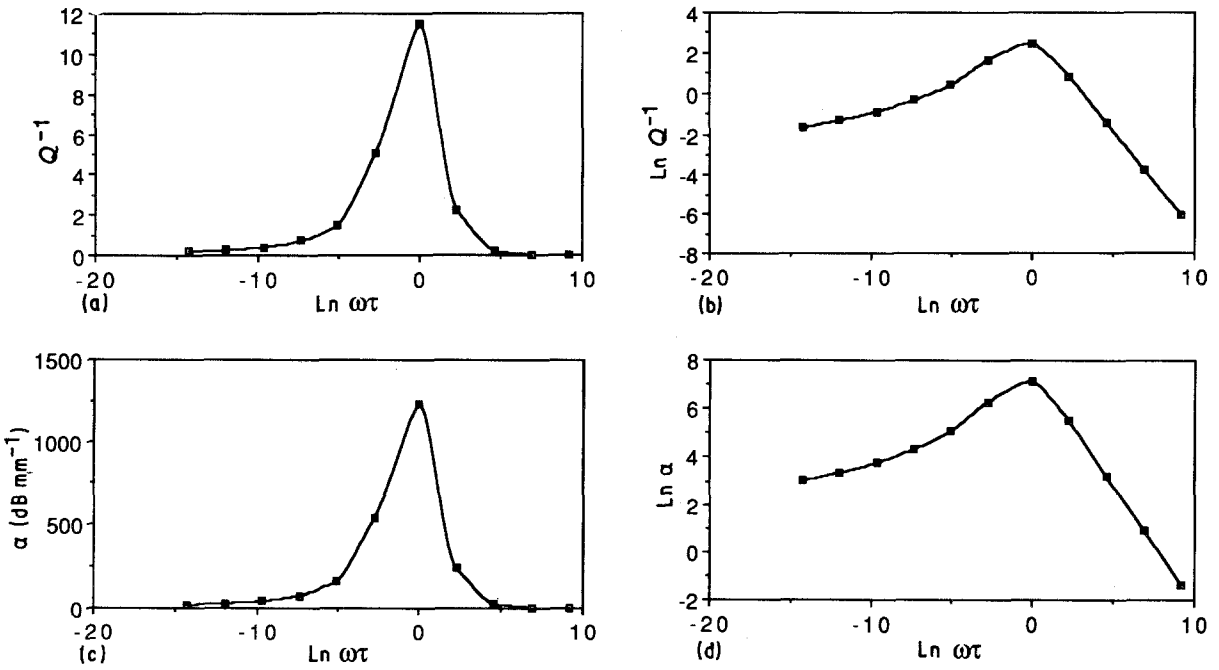

Figure 3. Theoretical upper bound to radiation-enhanced structural relaxation loss in polymethyl methacrylate, expressed as a function of angular frequency times the classical attempt period ($\omega\tau$) occurring in the two-well model of the loss. The bound has been obtained from a plot of Equations 19 and 20 with interpolation from those outside their range of accuracy. According to the model presented in the text, no matter how high the dose, the induced loss cannot exceed the bound. (a) Loss expressed as internal friction Q^{-1}, with a logarithmic plot of $\omega\tau$ data so that a readable presentation of the loss peak at $\omega\tau = 1$ is obtained on a single plot. (b) as (a), but expressed as a log–log plot for readable presentation of all Q^{-1} data on a single plot. (c) Loss expressed as attenuation coefficient $\alpha = \omega Q^{-1}/2c$, where c is the phase velocity, with a logarithmic plot of $\omega\tau$ as in (a). (d) As in (c) but expressed as a log–log plot as in (b). Over the range of the presented data the curve in (b) is represented very accurately by the polynomial fit

$$\ln Q^{-1} = 2.068 - 0.1495\ln\omega\tau - 0.1151(\ln\omega\tau)^2 - 0.0043(\ln\omega\tau)^3 + 5.948\times10^{-4}(\ln\omega\tau)^4 + 3.282\times10^{-5}(\ln\omega\tau)^5.$$

so that

$$Q_{\max}^{-1} = e^{-2}[\pi D^2 n/\rho c^2 kT(\ln\omega\tau)^2] \qquad (14)$$

where n is the number of loss centres per unit volume. It will become apparent later that we need to consider the case of $\omega\tau$ approaching unity and above. Under these conditions, Equations 12–14 become increasingly inaccurate with increasing $\omega\tau$. Under these conditions we must consider again the theoretical loss expression for an individual two-well system. Thus inspection of Equations 6 and 7 subject to the simplifying condition $\Delta = 0$, i.e. symmetric wells only, shows that Q^{-1} is a maximum with respect to variation of V under the condition

$$V_{\max} = -kT\ln\omega\tau \qquad (15)$$

Therefore, because V cannot be negative

$$V_{\max} = 0 \qquad \text{for } \omega\tau \geqslant 1 \qquad (16)$$

Because the concept of well asymmetry is meaningless for zero barrier heights, the initial neglect of asymmetry in obtaining Equation 15 is apparently inconsequential. Thus for $\omega\tau \geqslant 1$, the total Q^{-1} for n loss centres will be a maximum when

$$V \to 0 \qquad (17)$$

i.e. when the distribution function $n(v)$ is infinitely narrow, centred around $V \to 0$.

From the above discussion we thus find that

$$Q_{\max}^{-1} = (nD^2/4\rho c^2 kT)[\omega\tau/(1+\omega^2\tau^2)] \qquad \text{for } \omega\tau \geqslant 1 \qquad (18)$$

Equations 14 and 18 can be used to produce, by interpolation, the hypothetical variation of $Q_{\max}^{-1}$ with $\omega\tau$ over the entire range of $\omega\tau$ from 0–1. From Equation 10, taking for PMMA, $D = D_{\max} \approx 1$ eV, $\rho = 1171\ \text{kg m}^{-3}$, $c = 2600\ \text{m s}^{-1}$, $T = 293$ K, the temperature at which the experiments were carried out, and $n = n_a = 1.129\times10^{29}\ \text{m}^{-3}$ on the assumption that the maximum possible number of loss centres contributing to the loss is obtained by assuming one loss centre per atom, i.e. every atom can potentially reside in a two-well potential, one obtains

$$Q_{\max}^{-1} = 39\,(\ln\omega\tau)^{-2} \qquad \text{for } \omega\tau \ll 1 \qquad (19)$$

$$Q_{\max}^{-1} = 22.8\,\omega\tau/(1+\omega^2\tau^2) \qquad \text{for } \omega\tau \geqslant 1 \qquad (20)$$

To recapitulate the discussion of this section, the curve (Fig. 3) produced by interpolation from Equations 19 and 20 presents the theoretical upper bound to the internal friction that can be introduced in the sample regardless of how high the received dose is, for any $\omega\tau$, assuming, of course, that the sample remains intact and approximately homogeneous on a macroscopic scale, i.e. it does not cover the case of sample disintegration at extreme dose levels. It will become apparent that this curve is a suitable starting point for a discussion of the origin of the loss centres (τ values etc.) introduced in the present case.

Taking 10^{-13} s as the likely lower limit for τ, and $\omega = 2\pi\times10^7$, Equations 13 and 16 yield

$$V_{\max} = 0.151\text{–}0\ \text{eV} \qquad \text{for } \omega\tau = 2\pi\times10^{-6} \text{ to } \geqslant 1\ \text{s} \qquad (21)$$

Possible mean barrier heights in the normal (unirradiated) material span the range 1–70 kJ mol^{-1} corresponding to the hindered motion of various structural groupings [14], i.e. $0.725–7.25 \times 10^{-3}$ eV/formula unit, which is actually an individual barrier height because, in all cases, there is just one barrier site per formula unit. It will be noted that the value of V_{max} corresponding to $\tau = 10^{-13}$ s (which is a plausible attempt period for any of the above structural groupings), lies in the middle of this range.

From Fig. 3

$$Q_{max}^{-1} = 0.27–11.4$$

$$\text{for } \omega\tau = 2\pi \times 10^{-6} \text{ to } 1 \quad (22)$$

Because $Q^{-1} = 2c\alpha/\omega$, where α is the attenuation coefficient in Neper per unit length, where one Neper = 8.86 dB, we have

$$\alpha_{max} = 29–1221 \text{ dB mm}^{-1}$$

$$\text{for } \omega\tau = 2\pi \times 10^{-6} \text{ to } 1. \quad (23)$$

Thus here α_{max} is 23–977 times the value obtaining in the actual unirradiated sample. The first figure on the right-hand side of Equations 22 and 23 represents the maximum loss that can be achieved by means of the creation of two-well systems consisting of single atoms or small groups of atoms, i.e. $\tau \sim 10^{-13}$ s, whilst the second figure represents the maximum loss of all, i.e. the peak of the theoretical upper bound of the loss versus $\omega\tau$ curve. As explained in the next section, values of $\omega\tau$ corresponding to τ values orders of magnitude greater than 10^{-13} s must be associated with collective motions of large groups of atoms, e.g. entire chains. If the chains are sufficiently long so that $\omega\tau \gg 1$, a reasonable assumption for an unirradiated sample, inspection of Fig. 3 shows that the contribution to the overall loss produced by chain motion is small. Thus for the unirradiated sample we shall assume that the minimum possible actual number of loss centres expressed as a fraction of the total number of bonds, according to Equation 19, is

$$\alpha_{meas}/\alpha_{max}(\tau = 10^{-13} \text{ s}) = 1.25/29 = 0.043 = 4.3\% \quad (24)$$

This is a reasonable result and a good test of the theory thus far, because in a wide variety of amorphous materials, fractional values of n in the range 1%–3% are common [11, 12]. They are obtained through prior knowledge of V from $Q^{-1} - \omega - T$ plots information which is not available in the present case.

Now from the calculations of Section 3 we found that at the maximum dose level about 0.02% of bonds are ruptured and reformed. Clearly the probability of the radiation affecting the bonding associated with any one existing two-well system is extremely low: about $0.02 \times 0.4 = 0.008\%$. Thus the increased attenuation due to irradiation must be due to the creation of new two-well systems rather than the alteration of barrier heights and attempt frequencies of existing ones. If only two-well systems of atomic dimensions, i.e. $\tau \sim 10^{-13}$ s, were produced by the radiation, then on the reasonable assumption of one new two-well system per bond rupture, the theoretical attenuation increase at maximum dose would be

$$\Delta\alpha = \alpha(\text{normal sample}) \times \text{number of additional loss centres produced by the maximum dose/number of loss centres in normal sample}$$

$$= 1.25 \text{ dB mm}^{-1} \times 0.02/4.3$$

$$= 0.006 \text{ dB mm}^{-1} \quad (25)$$

This result is some 160 times too small to explain the observed increase which is 0.95 dB mm^{-1}. We conclude that many more atoms than the number of bond ruptures must be involved, in the loss mechanism enhanced by radiation. This implies the collective motion of large numbers of atoms rather than the motion of one or a few atoms across barriers of the order of one atomic width. Correspondingly, τ values much higher than 10^{-13} s are implied. A model of such a loss process is given in the next section.

6. A model of radiation-induced ultrasonic loss involving collective motions and low attempt frequencies

Consider a polymer chain containing a substantial number of formula units, though not so many that motion is impeded by intertanglement with other chains. There is the possibility of a collective translational motion of the chain against barrier heights much less than a bond ionization energy and over distances of the order of one atomic spacing. Because the chain as a whole can only reside in a single well, the collective motion will produce an internal friction loss as given by Equations 6 and 7 of the two-well model at the limit $V = \Delta = 0$ and taking the form

$$Q_c^{-1} = D_c^2 \omega\tau_c/4\rho c^2 kT(1 + \omega^2\tau_c^2) \quad (26)$$

where the subscript c denotes a chain property. Now in our chain model the possible maximum amplitude of the translational motion of each particle in the strain field is of the same order as that obtaining in a two-well system containing a single atomic particle, i.e. a significant fraction of one atomic spacing. Thus

$$D_c^2 = n_c D^2 \quad (27)$$

so that

$$Q_c^{-1} = n_c D^2 \omega\tau_c/4\rho c^2 kT(1 + \omega^2\tau_c^2) \quad (28)$$

where D is the deformation potential of the single particle two-well system (according to Equation 10 it has a maximum value of ≈ 1 eV in a polymer) and n_c is the number of atoms in the chain. To a first approximation the single well in which the chain moves may be assumed to be cubic with edges of length $L = (Mn_f/N\rho)^{1/3}$ where M, n_f, and N are the molecular formula mass, the number of formula units in the chain, and Avogadro's number, respectively. Correspondingly, the attempt period for the ground state is

$$\tau_c = 8mL^2/h = 8(Mn_f/N)^{5/3}/\rho^{2/3}h \quad (29)$$

where $m = Mn_f/N$ and L are the mass and length of the chain segment and h is Planck's constant. On average, the maximum radiation dose ruptures 1 in 5000 bonds and therefore, because there are two chain bonds in every formula unit of PMMA, sufficiently long molecular chains will be broken up into lengths containing 2500 formula units on average. Thus taking $\langle n_f \rangle = 2500$ and $M = 100$, one obtains $L = 7$ nm and $\langle \tau_c \rangle = 2.5 \times 10^{-4}$ s. Evidently values of n_f of only 8 would be needed to achieve the condition $\omega\tau = 1$. However, assuming Gaussian statistics, the frequency of occurrence of such chains induced by the radiation is much too small for them to make a significant contribution to the induced loss, notwithstanding the peak in the value of $\omega\tau/(1 + \omega^2\tau^2)$ at $\omega\tau = 1$. Integrating over all chain breaks, allowing for a distribution of chain lengths, the total induced loss can be expresed in the form

$$Q^{-1} = \int n(\tau_c) d\tau_c Q_c^{-1} \quad (30)$$

where $n(\tau_c)d\tau_c$ is the number of chains per unit volume with τ_c in the range τ_c to $\tau_c + d\tau_c$ and which thus contain n_c atoms. Thus

$$\int n_c n(\tau_c) d\tau_c = n_a \quad (31)$$

The variation (presumably of Gaussian form) of the distribution function about its peak value $n(\langle \tau_c \rangle)$ is much more rapid than the variation of the term $\omega\tau/(1 + \omega^2\tau^2)$, so that in the integration in Equation 30, to a first approximation, the term may be treated as a constant with $\tau_c = \langle \tau_c \rangle$. Thus for the total induced loss, Equations 28, 30 and 31 finally yield

$$Q^{-1} = (n_a D^2/4\rho c^2 kT)\omega\langle \tau_c \rangle/(1 + \omega^2 \langle \tau_c \rangle^2) \quad (32)$$

Substituting τ_c from Equation 29, for $\omega\tau \gg 1$, Equation 32 becomes

$$Q^{-1} = (n_a D^2 N^{5/3} h/32\rho^{1/3} c^2 kT\omega M^{5/3}) \langle n_f \rangle^{-5/3} \quad (33)$$

The loss thus takes the precise form of the Q_{max}^{-1}–$\omega\tau$ plot in Fig. 2 in the regime $\omega\tau > 1$ taking $\langle \tau_c \rangle = \tau$. In all the following calculations in this section, we take $\omega = 2\pi \times 10^7$ and the same values for D, ρ, c, T, and n_a are employed as were quoted just below Equation 18 and used to plot Fig. 2. Thus the predicted attenuation due to chain motion obtained by Equation 33 is given by

$$\alpha = 71344 \langle n_f \rangle^{-5/3} \text{ dB mm}^{-1} \quad (34)$$

As $\langle n_f \rangle$ increases in inverse proportion to the dose, Q^{-1} and α are thus proportional to the 5/3rd power of the dose. In Fig. 2 the solid line shows the theoretical variation of acoustic attenuation with dose predicted by Equation 34 when the latter is fitted to the experimental attenuation increase for the highest dose (0.95 dB mm^{-1}). The agreement of the theoretical curve with the experimental variation of attenuation is remarkable. The fit requires $\langle n_f \rangle = 841$ at the highest dose level. Such an average value of n_f would occur at dose levels 2500/841 = 3 times the actual (computed) highest dose level. Alternatively, substitution of $\langle n_f \rangle = 2500$ into Equations 29 and 34 gives $\tau = 2.49 \times 10^{-4}$ s, $\omega\tau = 1.57 \times 10^4$; and $\Delta\alpha = 0.156$ dB mm^{-1}, which is just one-half an order of magnitude less than the observed attenuation change. In another curve-fitting option it is possible to start with an assumption that the chain lengths prior to irradiation are finite. Assuming, as before, that the radiation does not affect the attenuation except through the mechanism proposed in this section (i.e. the two-well systems of atomic dimensions are unaffected), the attenuation change then predicted by Equation 34 is

$$\Delta\alpha = 71344(\langle n_f \rangle^{-5/3} - \langle n_f \rangle_0^{-5/3}) \text{ dB mm}^{-1} \quad (35)$$

where the subscript 0 denotes zero dose level. An exact derivation of the dose level dependence of $\langle n_f \rangle$ is now quite difficult, but intuitively, a reasonable first approximation is given by the formula

$$\langle n_f \rangle = (2500 \boldsymbol{D}_{max}/\boldsymbol{D}) \langle n_f \rangle_0 / (\langle n_f \rangle_0 + 2500 \boldsymbol{D}_{max}/\boldsymbol{D}) \quad (36)$$

where $\boldsymbol{D}$ is the dose, $\boldsymbol{D}_{max}$ is the maximum dose used, and the numerical factor of 2500 refers to the value of $\langle n_f \rangle$ that arises at the maximum dose level when $\langle n_f \rangle_0 = \infty$. Taking $\Delta\alpha = 0.95$ dB mm^{-1}, the maximum attenuation change, numerical solution of Equations 35 and 36 gives $\langle n_f \rangle_0 = 400$ and for the maximum dose $\langle n_f \rangle = 344$. The dose dependence predicted by Equations 35 and 36 on taking $\langle n_f \rangle = 400$ is approximately linear, and is thus a worse fit to the experimental data than we obtained by taking $\langle n_f \rangle = \infty$ earlier. Substitution of the $\langle n_f \rangle = 400$ in Equation 34 leads to a zero-dose attenuation of 3.3 dB mm^{-1}, which is 2.5 times greater than the observed value.

In view of the highly non-uniform dose field, and the strong (5/3 power) dependence of Q^{-1} on the dose, the above levels of agreement are good. Therefore, the final conclusion is that the radiation-induced losses are caused by collective atomic motions through approximately a significant fraction of one atomic spacing with vibrational frequencies of $\sim 4 \times 10^3$ Hz.

7. Applications

It will be useful to calculate the total dose, $\boldsymbol{D}$ (energy absorption), received by the specimen in the standard unit, i.e. the Gray (J kg^{-1}). The mass per mm^3 is 1.171×10^{-6} kg, so that given a mean ionization energy of 12 eV = 1.922×10^{-18} J, from Equation 4 we obtain

$$\boldsymbol{D} = 1.992 \times 10^{-18} N_i / 1.171 \times 10^{-6} = 36.5 \text{ kGy} \quad (37)$$

This result can be cross-checked from the application of a well-known rule of thumb that the exposure at 1 m from a 10 Curie ^{60}Co source is 0.2 roentgen min^{-1} [15] and in air the corresponding dose is 0.833 times the exposure, i.e. 1.66×10^{-3} Gy [16]. Thus at a distance of 7.5 mm over 24 h the dose in air would be $(10^6/7.5^2)(60 \times 24) 1.66 \times 10^{-3} = 42.5$ kGy. Because at ^{60}Co energies the beam attenuation coefficient is proportional to material density to a good approximation, for low atomic numbers, the energy absorption

per unit mass is almost independent of density. Thus the dose in all materials of low atomic number is approximately the same under identical conditions. This confirms the reliability of the full calculation (Equation 5) which agrees with the cross-check to within 14% (errors in the attenuation data are likely to be $\pm$ 5%).

According to standard sources ([3] p. 445, Table 4.38), plastic materials suffer only minor effects at doses of 100 kGy whilst at 1 MGy major damage occurs (50% effect) in the form of reduced strength, swelling, brittleness and gas evolution. So with a dosage used of only a third of the "minor effect" dose, yet with a pronounced, indeed large, change in ultrasonic properties (about ten times the minimum detectable change under the present operating conditions), it appears that ultrasonic monitoring is an extraordinarily sensitive indicator of radiation-induced structural change.

On-line ultrasonic monitoring could thus be a promising method of evaluating the effects of food irradiation. The destruction of bacteria alone would have little effect on ultrasonic attenuation levels but unwanted structural changes in the food products themselves could show up as an attenuation change. ^{60}Co radiation is used to kill micro-organisms, parasites, and insects in foodstuffs. Dosages of 0.03–0.15 kGy stop potatoes, onions and garlic from sprouting; 0.15–1 kGy is sufficient for disinfestation of grain, fruits, and vegetables; whilst 0.5–10 kGy is used for reducing spoilage microflora such as mould and vegetative bacteria [17]. These levels are below the lowest level of about 15 kGy at which an ultrasonic change first became discernible in the present experiment, which is how they should be. The polymer employed is more or less identical to any foodstuff from the standpoint of interaction with radiation and one might set 15 KGy as a threshold level above which food treatment should not take place, because structural changes in the food itself, not just in the live contaminants, are likely to be taking place.

Acknowledgements

The use of radiation facilities and the technical assistance of Mr S. Joshi, Physics Department, Brunel University, are gratefully acknowledged in respect of the experimental part of this paper.

References

1. I. G. RITCHIE, J. F. DUFRESNE and P. MOSER, in "Internal Friction and Ultrasonic Attenuation in Solids", edited by C. C. Smith (Pergammon Press, 1979) pp. 43–7.
2. D. BERETZ, M. HALBWACHS and J. HILLAIRET, *ibid.*, pp. 131–8.
3. P. B. FRASER, in "Physical Acoustics", Vol. V, edited by W. P. Mason (Wiley, 1972) Ch. 2, pp. 59–109.
4. R. E. STRAKNA, *Phys. Rev.* **123** (1961) 2020–6.
5. A. CALLENS, R. DE BATIST and R. GIVERS, in "Internal Friction and Ultrasonic Attenuation in Solids", edited by C. C. Smith (Pergammon Press, 1979) pp. 255–60.
6. B. BRIDGE, F. HARIRCHIAN, D. C. IMRIE, Y. MEHRABI and A. R. MERAGI, *NDT Int.* **20** (1987) 339.
7. R. A. BOLZ and G. L. TUVE, (eds), "Handbook of tables of Applied Engineering Science", 2nd Edn (CRC Press, Boca Raton, FL) Table 4.32, Section 4.2, p. 441.
8. G. W. C. KAYE and T. H. LABY (eds), "Handbook of Physical and Chemical Constants", 14th Edn (Longman, London, New York) Section 3.4.2, p. 277.
9. B. BRIDGE, *J. Photographic Sci.*, **34** (1986) 95.
10. *Idem, Brit. J. NDT.* **28** (1986) 216.
11. B. BRIDGE and A. A. HIGAZY, *J. Mater. Sci.* **23** (1988) 1995.
12. B. BRIDGE and N. D. PATEL, *ibid.* **21** (1986) 3783.
13. K. S. GILROY and W. A. PHILLIPS, *Phil. Mag. B* **43** (1981) 735
14. B. BRIDGE, B. GABRYS, S. JOSHI and J. HIGGINS, *J. Mater Sci.* **24** (1989) 3295.
15. R. HALMSHAW, in "The physics of industrial radiology", edited by R. Halmshaw, (Heywood, London, American Elsevier, New York, 1966) Ch. 1, p. 16.
16. *Idem*, "NonDestructive Testing", (Edward Arnold 1987) Section 3.3.4, p. 31.
17. A. BRYNJOLFSSON, in "Concise Encyclopaedia of Science and Technology", edited by S. B. Parker (McGraw-Hill, New York, 1982) pp. 740–1.

Received 10 January
and accepted 4 February 1992